Check for updates

www.advmattechnol.de

Counting All Photons: Efficient Optimization of Visible Light 3D Printing

Lynn M. Stevens, Elizabeth A. Recker, Kevin A. Zhou, Vincent G. Garcia, Keldy S. Mason, Clotilde Tagnon, Nayera Abdelaziz, and Zachariah A. Page*

The utility of visible light for 3D printing has increased in recent years owing to its accessibility and reduced materials interactions, such as scattering and absorption/degradation, relative to traditional UV light-based processes. However, photosystems that react efficiently with visible light often require multiple molecular components and have strong and diverse absorption profiles, increasing the complexity of formulation and printing optimization. Herein, a streamlined method to select and optimize visible light 3D printing conditions is described. First, green light liquid crystal display (LCD) 3D printing using a novel resin is optimized through traditional empirical methods, which involves resin component selection, spectroscopic characterization, time-intensive 3D printing under several different conditions, and measurements of dimensional accuracy for each printed object. Subsequent analytical quantification of dynamic photon absorption during green light polymerizations unveils relationships to cure depth that enables facile resin and 3D printing optimization using a model that is a modification to the Jacob's equation traditionally used for stereolithographic 3D printing. The approach and model are then validated using a distinct green light-activated resin for two types of projection-based 3D printing.

1. Introduction

Additive manufacturing (3D printing) has entered industrial, academic, and consumer sectors, due to the combination of high speed, material versatility, and geometric precision relative to conventional subtractive manufacturing and injection molding processes.^[1–3] Although impressive advancements in 3D printing technology have been made in recent years, a number of opportunities remain to further expand the range of printable materials (e.g., composites and biomaterials), while simultaneously optimizing production rate and feature resolution at an affordable price. To this end, vat photopolymerization represents one of the most modular 3D printing techniques.

L. M. Stevens, E. A. Recker, K. A. Zhou, V. G. Garcia, K. S. Mason, C. Tagnon, N. Abdelaziz, Z. A. Page Department of Chemistry
The University of Texas at Austin
105 East 24th Street, Stop A5300, Austin, Texas 78712, USA
E-mail: zpage@cm.utexas.edu

The ORCID identification number(s) for the author(s) of this article can be found under https://doi.org/10.1002/admt.202300052

DOI: 10.1002/admt.202300052

In vat photopolymerization, rapid solidification of a liquid resin occurs upon exposure to light (i.e., photocuring) in specific, predefined locations,[4,5] reconstructing computer-generated 3D objects in a layer-by-layer fashion. Although different optical exposure mechanisms exist, from point-by-point laser rastering for stereolithography (SLA) to 2D projection for digital light processing (DLP) and liquid crystal display (LCD) technology, they share a common utility of high energy UV to violet light (≤405 nm) to achieve rapid curing.[6-8] However, reliance on UV-violet light limits resin components to those with minimal interactions in that spectral region, where molecular absorption and scattering are pervasive. [9-12] Furthermore, LCDs are damaged by prolonged UV light exposure (<400 nm), making visible light curing particularly attractive for LCD 3D printing (Figure 1A), which is one of the least expensive and most scalable technologies (i.e., large build areas).[13,14]

For UV-violet (\leq 420 nm) light, Type I photocuring dominates, where light absorption and polymerization initiation occurs by a single molecule (photoinitiator). Conversely, visible light-based 3D printing at wavelengths longer than \approx 450 nm (blue) necessitates the use of a multicomponent photosystem that operates by a so-called Type II mechanism. Type II relies on distinct molecules for absorption (dye) and initiation (initiator). This arises from the requirement for a symmetry forbidden high-energy n π^* transition by UV-violet light to cause bond scission and radical formation (Type I), while low-energy visible-to-near infrared (NIR) photons cause π π^* transitions and do not typically break bonds. Instead, dye excitation via π

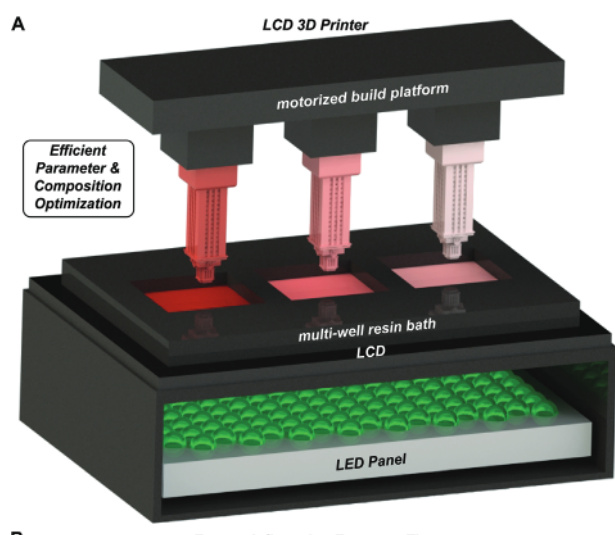
 π^* followed by electron transfer (redox) between the dye and nitiator molecules facilitates radical formation and curing (Type II, **Figure 2A**). A common consequence of symmetry-allowed excitation via π π^* transitions is a large molar absorptivity (\approx 50 000-200 000 M 1 cm 1) relative to n π^* (<10 000 M 1 cm 1), which increases the likelihood of redox occurring per incident visible photon. Despite this, the bimolecular nature of Type II photosystems often results in slower photocuring relative to Type I photosystems, precluding its widespread implementation in rapid projection-based 3D printing (e.g., DLP and LCD).

2365709x, 2023, 23, Downloaded from https://onli

elibrary.wiley.com/doi/10.1002/admt.202300052 by University Of Texas Libraries.

, Wiley Online Library on [08/05/2024]. See the Terms and Conditions (https://onlinelibrary.wiley.com/terms

conditions) on Wiley Online Library for rules of use; OA articles are governed by the applicable Creative Commons



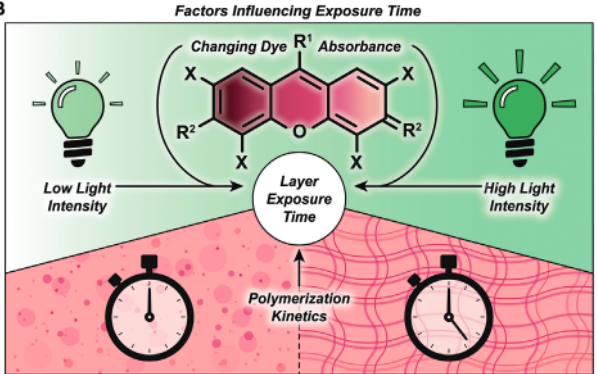


Figure 1. Overview of LCD 3D printing protocol and optimization. A) Rendering of multiwell, green LED containing LCD 3D printer and B) overview of the parameters that influence resolution and slice exposure time discussed herein.

Recently, we discovered three-component (Type II) photosystems and oxygen scavenging additives that enabled rapid (build speeds at 33–45 mm hr 1), visible to NIR ($\lambda_{\rm max}=470-850$ nm; intensity, $I\approx 2–5$ mW cm 2), high resolution (<100 µm lateral; 25 µm vertical) DLP 3D printing under ambient conditions, competitive with commercially available UV-violet light (Type I) curing. [19–22] The desire to translate visible light reactive resins to LCD 3D printing and simultaneously facilitate resin diversification for a wider material scope motivated a mathematical approach to identify exposure conditions for optimal speed and resolution. In this regard, the Jacob's equation has served as a standard model to predict exposure time per layer for vat photopolymerization 3D printing (Equation 1)[23]:

$$C_{\rm d} = D_{\rm p} \ln \left(\frac{E}{E_{\rm c}} \right) \tag{1}$$

where cure depth (C_d) is related to the depth of light penetration into the resin (D_p) – defined as the depth at which the incident irradiance (I_0) on the resin decreases to 37% of its initial value – the energy dosage of light for a given layer (E), and the critical energy dose of light to form an infinitesimally small gel (E_c). For conventional Type I photocuring in SLA systems, this model has

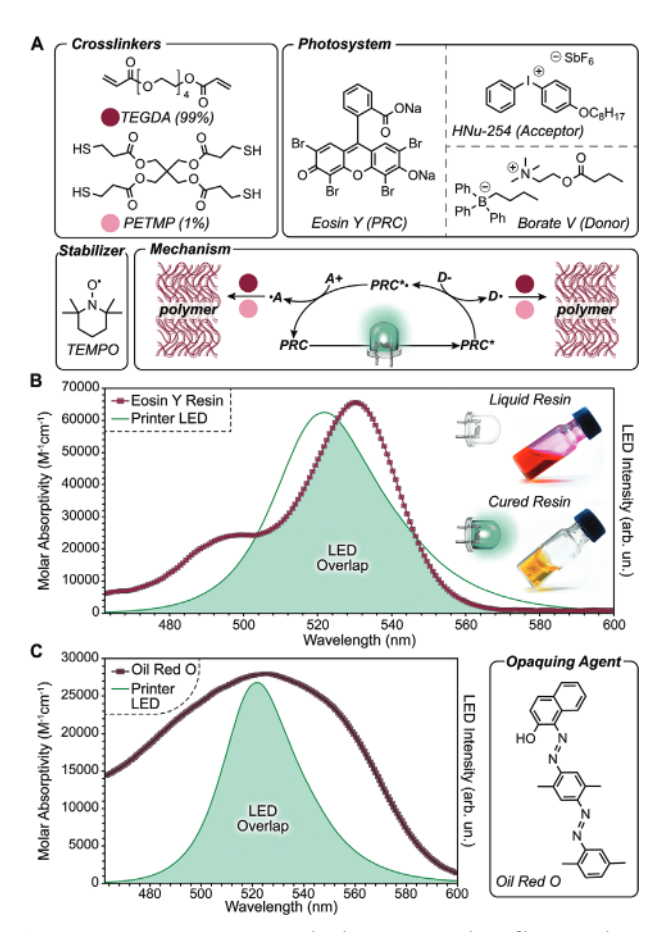


Figure 2. Resin composition and relevant spectral profiles. A) Chemical structures of crosslinkers, photosystem components (EY = 0.1 wt.%, HNu-254 = 2 wt.%, Borate V = 0.2 wt.%), and stabilizer (0.01wt.%), along with a general Type II PRC photopolymerization mechanism. B) Overlay of EY absorbance profile, obtained in TEGDA:PETMP resin, with printer green LED profile; overlapping area shaded in green and inset vials showing pre- (top) and post- (bottom) green LED exposure. C) Overlay of Oil Red O, opaquing agent (OA), absorbance profile, obtained in TEGDA/PETMP resin, with printer green LED profile (left) and chemical structure of OA (right).

been shown as a useful strategy to optimize experimental printing conditions (exposure time per layer). However, the Jacob's equation does not consider "higher-order" effects including optical self-focusing, resin bleaching, heating, and scattering, [24,25] which are known to influence resolution (Figure 1B). [23] In turn, researchers have pursued modifications to the Jacob's equation to account for "sublinear" behavior in SLA resins due to oxygen inhibition among other factors. [26] However, a working curve has not explicitly been developed for Type II vat photopolymerization resins, presenting an opportunity for optimization of visible light 3D printing.

Herein, green light LCD 3D printing was demonstrated for the first time, along with a systematic examination of higher-order effects on resolution, providing a streamlined method and modified Jacob's equation, termed the Recker–Jacob's equation, for determining ideal printing conditions. This was accomplished using a model Type II photosystem, a custom LCD 3D printer equipped with a multiwell vat (Figure 1A), Fourier transform

ADVANCED MATERIALS

2365790x, 2023, 23, Downloaded from https://onlinelibrary.wiley.com/doi/10.1002/admt.2023.00052 by University Of Texas Libraries, Wiley Online Library on [08092024]. See the Terms and Conditions (thtps://onlinelibrary.wiley.com/terms-and-conditions) on Wiley Online Library for rules of use; OA articles are governed by the applicable Creative Commons.

infrared and UV-visible absorption spectroscopies to monitor photo-polymerization and bleaching kinetics, photorheology to experimentally determine gel points (E_c), optical profilometry, scanning electron microscopy (SEM), and computed tomography (CT) scanning to characterize part resolution. Finally, the utility of the Recker-Jacob's equation to predict optimal printing conditions was validated using a novel green-light sensitive resin composition.

2. Results and Discussion

A model Type II photosystem activated by a green LED $(\lambda_{max} = 525 \text{ nm})$ was initially developed for 3D printing with a custom LCD system. The resin comprised tetraethylene glycol diacrylate (TEGDA, 99 wt.%) as an amphiphilic crosslinker to facilitate solubility of photosystem components, pentaerythritol tetrakis(3-mercaptopropionate) (PETMP, 1 wt.%) to enable 3D printing in the presence of oxygen (previously reported),[21] and 2,2,6,6-tetramethylpiperidine 1-oxyl (TEMPO, 0.005 wt.%) as a radical scavenger to improve resin stability and mitigate curing outside irradiation zones (Figure 2A, Figure S1, and Tables S1 and S2, Supporting Information). To achieve rapid photocuring, the photosystem selected comprised [4-(octyloxy)phenyl](phenyl)iodonium hexafluoroantimonate (HNu-254, 2 wt.%) and 2-(butyryloxy)-N,N,Ntrimethylethan-1-aminium butyltriphenylborate (Borate V, 0.2 wt.%) as a strong electron acceptor (A) and donor (D) pair,[20-22] respectively, and Eosin Y disodium salt (EY) as the photoredox catalyst (PRC, 0.1 wt.%), due to its high molar absorptivity and profile that closely overlapped with the green LED profile on the LCD 3D printer (Figure 2A,B). Absorbance (A) of EY dissolved in the TEGDA:PETMP (99:1) resin was measured at the planned initial printing conditions based on related precedent^[21] (0.1 mol%, concentration, c = 1.6 mM). This was accomplished by passing a UV-vis probe light through a thin solution of the resin sandwiched between glass slides with a defined gap thickness (l) of 25, 38, 51, 76, or 102 µm (see Section 2.2. in the SI for further details). Under these conditions, the peak absorption (λ_{max}) for EY was 530 nm, giving a peak molar absorptivity () of 65 600 M ¹ cm ¹ (Figure 2B, Figure S5, Table S3, Supporting Information) as determined using the Beer-Lambert Law (Equation 2):

$$A = l\varepsilon c \tag{2}$$

Next, three azo-dyes were examined – Sudan I, Oil Red O, and Sudan Black – to serve as opaquing agents (OAs) that mitigate cure-through by passively attenuating light in the z-direction, and ideally confine the depth of cure to a \approx single layer. For clarity, the discussion focuses on the use of Oil Red O given its optimal absorption overlap with both EY absorption and LED emission profiles (Figure 2C, see SI Section 3.1. for additional details on alternative OAs). As an initial screen, this photoredox system (in the absence of OA) was shown to rapidly cure when exposed under ambient conditions to green light (\approx 525nm) at the highest printer intensity on the present system (<10 s to gelation at 6.4 mW cm 2) (Figure 2B, vial inset).

Formulation optimization was accomplished using real-time Fourier transform infrared spectroscopy (RT-FTIR) to characterize the rate of acrylate conversion to polymer by monitoring the disappearance of the C≐C stretch at 3100 cm⁻¹ during irradiation (Figure 3A).[27] The effect of green light intensity at the predefined printer values of 1, 2.4, 4.4, and 6.4 mW cm² was found to directly correlate with the apparent rate of polymerization (k_n^{app}) for resins containing no OA, increasing from 10.1 ± 0.9 , $16.8 \pm$ 0.2, 22.4 \pm <0.1, to 27.8 \pm 0.5%/s, respectively (Figure S13 and Table S4, Supporting Information). Of note, given a small difference in spectral output between the LEDs on the LCD 3D printer and the LEDs used for experimentation, the intensities for the latter were adjusted to 0.91, 2.25, 4.23, and 6.30 mW cm² to match the number of photons absorbed by the present photosystem (see Section 3.4 in the SI for more details). At each intensity, the effect of [OA] on k_n^{app} was examined using 0.0025, 0.005, 0.01, 0.015, and 0.025 wt.% OA relative to crosslinker. It was found that as [OA] increased, $k_{\rm p}^{\rm app}$ decreased (Figure 3A). Photorheology confirmed that under these conditions rapid photopolymerization occurs, with gel points ranging from 3.9-13.6 s depending on the light intensity and [OA] used (Figure S34-S35 and Table S8, Supporting Information). Overall, these curing speeds are compatible with projection-based 3D printing and competitive with industry standards, having particular utility in LCD 3D printing given the often-low operating intensities (<5 mW cm⁻²).

Printing optimization was accomplished using a custom multiwell vat and corresponding build platform (Figure 1A and Figure S4, Supporting Information), where six different resin formulations could be tested simultaneously. By this method, both lateral (x,y) and vertical (z) resolution were optimized by varying light intensity, [OA], and exposure time per 50 µm layer (Figure 3B,C). Using a time-based "resolution print" that contains arrays of small square features it was qualitatively determined that increasing [OA] from 0 to 0.025 wt.% improved resolution, but at the cost of longer exposure times (Figures S36, Supporting Information). Notably, reproducible printing at [OA]'s >0.025 wt.% was challenging, likely due to large light attenuation, mitigating a complete cure through the depth of a single layer (50 µm) (Figure S37, Supporting Information). Based on these findings, to quantitatively determine the effect of light intensity on lateral resolution resins containing 0.025 wt.% OA were employed to 3D print square pegs with varying dimensions from two pixels (100 µm) to 32 pixels (1600 µm) wide at the four different light intensities while maintaining a light dosage of 35 mJ by varying exposure times from 5.5 to 35 s/50 µm layer in going from 6.4 to 1 mW cm⁻², respectively (Figure 3B, Figure S38, and Table S9, Supporting Information). Characterizing the top surface area of each 32-, 16-, and 8-pixel wide square using optical profilometry and comparing to theoretical values revealed a $>2\times$ decrease in percent over-cure for prints prepared using 6.4 mW cm⁻² relative to those using 1 mW cm⁻² (Figures S39-S42, Tables S10-S12, and Equation S1, Supporting Information). The improvement in lateral resolution when using higher light intensities was hypothesized to arise in-part from faster curing and, in-turn, reduced mixing (i.e., blurring) at the interface.

With an optimal light intensity of 6.4 mW cm², the effect of [OA] and exposure time per layer on *z*-resolution (i.e., "cure-through") was quantified using a 3D print containing bridges with horizontal sections having a theoretical thickness of 750 µm (i.e., 15 layers) (Figure 3C and Figures S43-S44, Supporting Information). Vertical cure-through on the horizontal sections was directly measured using optical profilometry. Without OA, the

2365709x, 2023, 23, Downloaded from https://onlinelibrary.wiley.com/doi/10.1002/admt.202300052 by University Of Texas Libraries

, Wiley Online Library on [08/05/2024]. See the Terms

-and-conditions) on Wiley Online Library for rules of use; OA articles are governed by the applicable Creative Commons

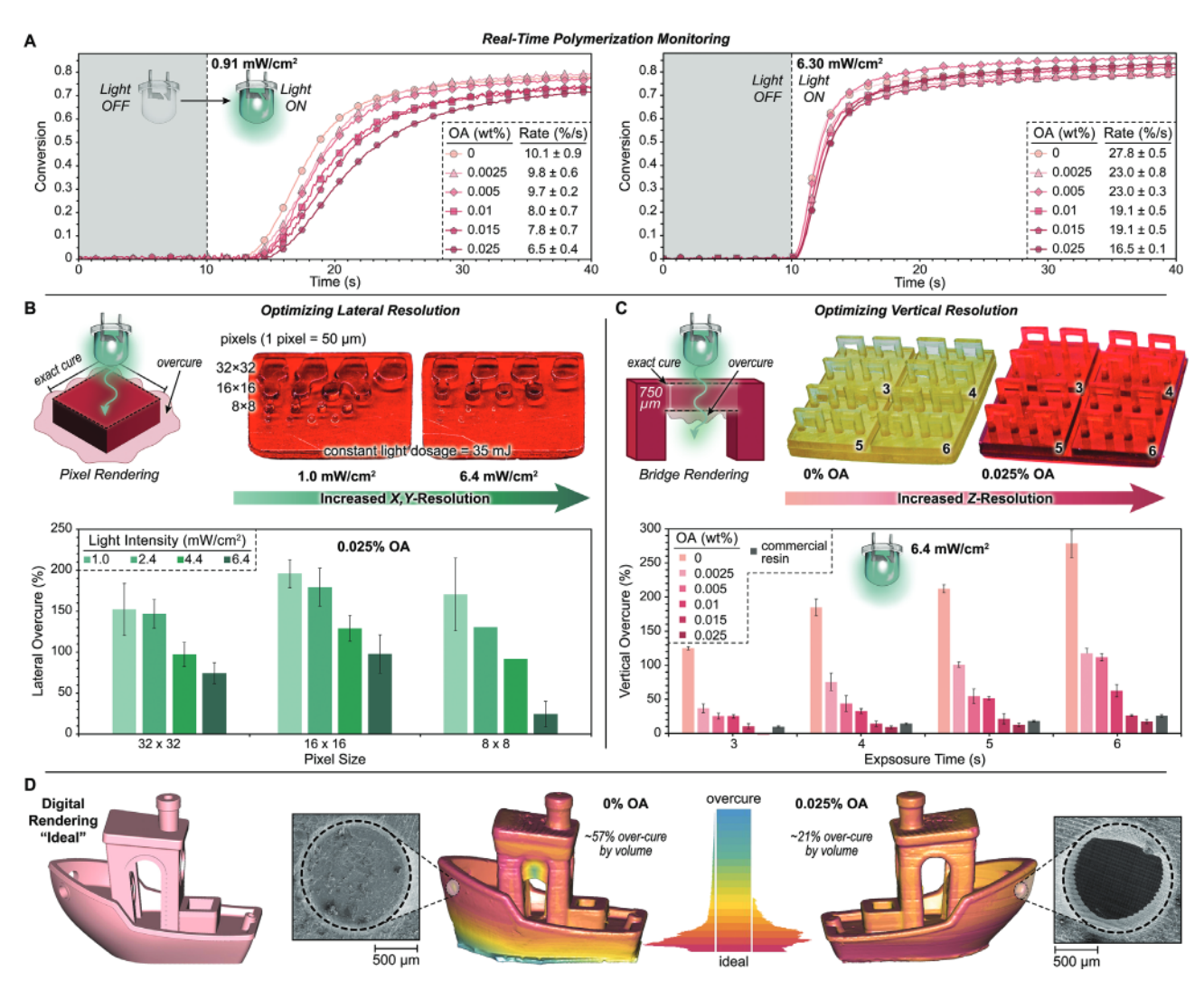


Figure 3. Empirical optimization of lateral and vertical resolution by varying light intensity, [OA], and exposure time per 50 μm layer. A) Monitoring conversion of crosslinker to polymer in real time using photo-FTIR spectroscopy, varying [OA] from 0 to 0.025 wt.% and LED intensity from 0.91 mW cm 2 (left) to 6.30 mW cm 2 (right). Symbols have been indexed by 10 for clarity. B) Schematic representation of a 3D printed square showing lateral over-cure (left) and photographs of 3D printed square arrays (right) produced from resins containing 0.025 wt.% OA, while varying light intensity from 1.0 to 6.4 mW cm 2 . Bar graph provides an average percent lateral over-cure for three different sized square blocks produced at the four different intensities. Error bars represent ±1 standard deviation from the mean. (C) Schematic representation of a 3D printed bridge showing vertical over-cure (left) and photographs of 3D printed bridge arrays (right) produced using a light intensity of 6.4 mW cm 2 from resins with [OA]'s ranging from 0 to 0.025 wt.% and exposure times from 3 to 6 s per layer. Bar graph provides an average percent vertical over-cure for the different conditions. Error bars represent ±1 standard deviation from the mean. D) Calibration test print of "3DBenchy" showing reconstructed 3D images from CT scans and SEM images of the portholes. Prints were produced using resins with no OA (center) and 0.025 wt.% OA (right), at an intensity of 6.4 mW cm 2 . The colored bar represents over-cure generated by overlaying the CT scan and digital print file, with histograms pointing in the direction of the corresponding prints showing normalized distances of printed voxels from their theoretical position in the digital file.

percent over-cure ranged from $126 \pm 2\%$ to $280 \pm 21\%$ for 3 and 6 s per layer exposure times, respectively (Figure 3C and Table S13, Supporting Information). Increasing [OA] led to a dramatic decrease in percent over-cure, culminating in a near perfect match to theoretical for 0.025 wt.% OA at an exposure time of 3 s per layer (i.e., 0% over-cure) and $18 \pm 3\%$ for 6 s per layer. This *z*-resolution was competitive with that obtained for the same bridges printed with 405 nm LCD light from a commercial resin meant to provide detailed features (B9R-2-Black Resin from B9 Creations) (Figure 3C, Figure S45, and Table S13, Supporting Information).

To test the optimized conditions, a modern resolution calibration file, 3DBenchy, was printed for resins without and with 0.025 wt.% OA at an exposure time of 5 s per layer and an intensity of 6.4 mW cm ² (Figure 3D). Characterization with SEM and CT scanning showed the combined improvement in both lateral and vertical resolution by incorporating OA. This was clearly evident by the presence of the small and overhung porthole when using OA, along with the decrease in volumetric over-cure from 57% to 21%, as estimated from the CT scan 3D reconstruction compared to the original digital file (Figure S54, Supporting Information). The remaining over-cure was hypothesized to be due in-part to

ADVANCED MATERIALS TECHNOLOGIES 2365709x, 2023, 23, Downloaded from https://onlinelibrary.wiley.com/doi/10.1002/admt.202300052 by University Of Texas Libraries, Wiley Online Library on [0805/2024]. See the Terms and Conditions

) on Wiley Online Library for rules of use; OA articles are governed by the applicable Creative Commons

thermal effects that arise from the rapid exothermic polymerizations (Figures S60-S63, Supporting Information). However, further quantification of this effect is required to correlate it with print fidelity. Overall, it was observed that good x-, γ -, and z-resolution can be achieved with the proper combination of light intensity, [OA], and exposure time per layer.

After performing an empirical optimization of LCD 3D printing, it was apparent that the ambiguity of selecting an ideal [OA] and exposure time per layer results in time- and materialintensive experimentation. This motivated efforts to streamline the optimization process by modifying the standard Jacob's working curve (Equation 1). To start, the green LED emission spectrum was recorded from the front of the LCD screen on the 3D printer and overlaid with EY's molar absorptivity profile (Figure 2B). Although the green LED on the printer is centered at 521 nm for an intensity of 6.4 mW cm⁻², in contrast to a laser, the spectral output spans across a range of wavelengths, specifically from ≈465-615 nm with a full width at half maximum (FWHM) of \approx 35 nm. Thus, it was pertinent to consider all photons absorbed by calculating an average molar absorptivity (avg) based on the overlap between the LED emission and EY absorption profiles, as opposed to using the molar absorptivity at 521 nm. This actinometric-type quantification began by normalizing the LED emission profile such that the area under the curve was equal to the total intensity of light as measured by a silicon photodiode power sensor at the four different printing conditions used in this study: 1, 2.4, 4.4, and 6.4 mW cm⁻² (Section 3.12. in the SI for additional details). The total number of photons (n) for each intensity of light was then calculated based on Equations 3A and 3B:

$$E = \frac{hc}{\lambda} \tag{3A}$$

$$W = n \frac{E}{s} \tag{3B}$$

where E= energy (J), h= Plank's constant ($\approx 6.6 \times 10^{-34}$ J·s), and c= speed of light ($\approx 3 \times 10^8$ m s $^{-1}$). Given the LED emission profiles in number of photons per nm for the four different intensities, avg of EY was calculated by taking the sum of photon fraction per nm multiplied by the corresponding value. This transformation provided avg values of $\approx 41,700-41,300$ M $^{-1}$ cm $^{-1}$ for EY and 25 700—25 400 M $^{-1}$ cm $^{-1}$ for OA (Oil Red O) (Table S14, Supporting Information). The subtle variability arises from small spectral shifts in the emission profiles for different printer LED intensities (see Section 3.4. and Table S7 in the Supporting Information).

Given high $_{\rm avg}$ values for both EY and the OA (Oil Red O), it was important to take both into account, converting Equation 2 into Equation 4:

$$A = l\left(\varepsilon_{EY}[EY] + \varepsilon_{OA}[OA]\right) \tag{4}$$

where [EY] is the concentration of Eosin Y and [OA] is the concentration of Oil Red O. However, upon irradiation of the resin a stark change in color (and thus A) was observed. For example, in the absence of OA the resin went from red/pink to near colorless in <30 s of exposure to the green LED (6.3 mW cm 2), which is a time-scale comparable with photocuring (**Figure 4**A, inset). Thus, this higher-order photobleaching effect, not considered by

the standard Jacob's equation, was deemeded necessary to consider for the present photosystem. It is noteworthy that photobleaching during photocuring is not uncommon, and can be advantageous in controlling the color (or lack of color) of the final part. [24] To this end, photobleaching was tracked by UV-vis absorption spectroscopy to quantify the change in effective [EY] as a function of irradiation intensity (Figure 4A, see Section 3.13. in the SI). Samples were 50 μm thick between glass slides to match the thickness of one layer on the LCD 3D printer. Photobleaching was found to follow first order kinetics, and was thus attributed to degradation of EY over time (Equation 5, Figure 4B, Figures S68–S79, and Table S15, Supporting Information).

$$[EY]_t = [EY]_0 e^{-kt}$$
(5)

where $[EY]_t$ is the concentration of Eosin Y at time t, $[EY]_0$ is the concentration of Eosin Y at t = 0 (1.6mM), and k is the photobleaching rate constant. Control experiments confirmed no photobleaching of the OA, allowing for [OA] to be treated as a constant (Figure S67, Supporting Information). Plugging Equation 5 into Equation 4 provides the time dependent equation for A that considers photobleaching kinetics (Equation 6):

$$A = l \left(\varepsilon_{EY} \left([EY]_0 e^{-kt} + \varepsilon_{OA} [OA] \right) \right)$$
 (6)

where $_{\rm EY}$ and $_{\rm OA}$ represent $_{\rm avg}$ for EY and the OA, respectively, which accounts for the overlap between their absorption profiles and the LED emission profile.

To translate these findings to 3D printing parameters, A can be correlated to photocuring by recognizing that C_d is simply the pathlength that a sample of resin will cure through at a given energy, and thus it can be equated to length (l) from the Beer-Lambert Law (Equation 2) for a defined layer that is being cured during the printing process. Plugging this into Equation 6 and solving for C_d provides Equation 7.

$$C_d = \frac{A}{\varepsilon_{FY} \left([EY]_0 e^{-kt} + \varepsilon_{OA} [OA] \right)}$$
 (7)

where *A* can be replaced in-terms of its relationship to energy (see Equations S5 and S6 for derivation), which provides Equation 8 (Recker-Jacob's Equation):

$$C_{d} = \frac{\log\left(\frac{E}{E_{c}}\right)}{\varepsilon_{EY}\left([EY]_{0}e^{-kt} + \varepsilon_{OA}[OA]\right)}$$
(8)

To use Equation 8 in practice for a different resin would require measuring photobleaching kinetics, -k, as shown in Figure 4B, which, although less material intensive, is still somewhat time intensive. However, plotting -k vs. LED intensity, I, for the present resin revealed a linear relationship with a slope of -0.042 ± 0.005 , irrespective of the [OA] used (Figure 4C, Equation 9, and Figure S80, Supporting Information).

$$k = 0.042I \tag{9}$$

It is hypothesized that the independence on [OA] occurs when resin absorption remains low (e.g., $A \le 1$), as is the case here (Figure S81, Supporting Information). Thus, by meeting this

2365709x, 2023, 23, Downloaded from https://onli

rary.wiley.com/doi/10.1002/admt.202300052 by University Of Texas Libraries

, Wiley Online Library on [08/05/2024]. See the Terms and Conditions (https://onlinelibrary.wiley.com/terms

conditions) on Wiley Online Library for rules of use; OA articles are governed by the applicable Creative Commons License

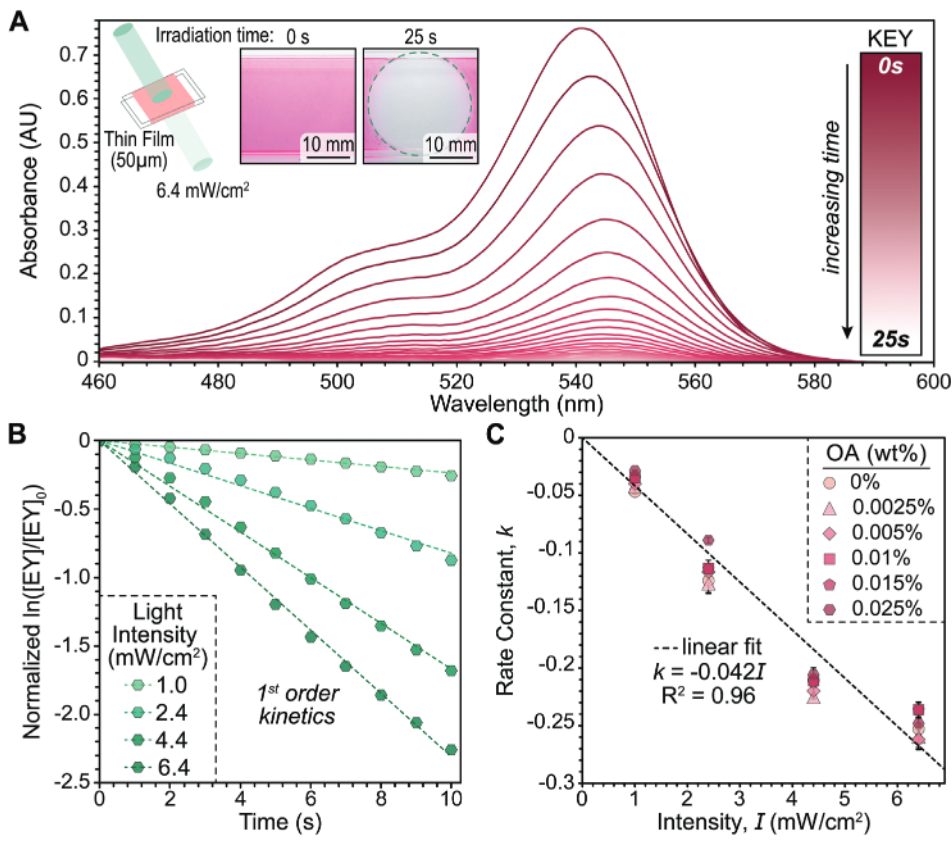


Figure 4. Photobleaching studies. A) Representative UV-vis absorbance plot of a resin containing EY and Oil Red O (OA, 0.025 wt.%) upon exposure to a green LED at 6.3 mW cm⁻². For clarity, samples were baselined with OA (0.025 wt.%) and the inset shows a sample with no OA under otherwise identical conditions. B) First-order kinetic fitting for photobleaching trials at varying light intensity. C) Linear relationship between photobleaching rate constant(-k) and light intensity.

condition ($A \le 1$), a photobleaching measurement for one resin condition (i.e., no OA or one [OA]) would be the only requirement, greatly reducing the total amount of necessary experimentation. Furthermore, with the relationship between -k and I, the Recker-Jacob's equation can be simplified to Equation 10 where C_d for a given resin can be modeled solely in terms of E, P, and P.

$$C_{d} = \frac{\log\left(\frac{E}{E_{c}}\right)}{\varepsilon_{EY}\left([EY]_{0}e^{-0.042(E)} + \varepsilon_{OA}[OA]\right)}$$
(10)

To compare theory to experiment, $C_{\rm d}$ was measured using a rheological technique recently developed by Williams and coworkers^[28] that enables quantification under printing relevant conditions; layer thicknesses <500 µm and exposure times <60 seconds. Based on this method,^[28] a force of 2N was identified as the threshold for cured material with the present resin (see Section 2.5 in the Supporting Information for more details). Comparing the experimental results to curves generated from the original Jacob's equation revealed a stark underprediction of $C_{\rm d}$ (Figure 5A and Figures S83, Supporting Information). In contrast, the Recker-Jacob's equation provides a much better prediction, which is attributed to the consideration of avg instead of max, along with accounting for photobleaching. Based on prior printing optimization (Figure 3) it was empirically determined

that for resins containing 0.025 wt.% OA an exposure time of \approx 4-5 seconds per 50 µm layer consistently provided prints with good z-resolution; <20% over-cure, equal to a tolerance of \approx 10 µm. This exposure time range corresponds to a predicted $C_{\rm d}$ of \approx 80–135 µm, which is notably larger than the \approx 60 µm layers experimentally observed (i.e., \approx 10 µm over-cure). This discrepancy may be attributed to the 2 N force condition used to determine $C_{\rm d}$, where a larger force threshold would be anticipated to provide more comparable values. Regardless, given these conditions, a target $C_{\rm d}$ of \approx 100 µm (i.e., \approx 2× the printing layer thickness) can be used to predict the ideal exposure time per layer.

The same rheological method was employed to determine the effect of [OA] on $C_{\rm d}$ at the highest LED intensity (6.3 mW cm 2). In all cases, the Recker-Jacob's equation was found to provide a good fit to the data (Figure 5B and Table S16, Supporting Information). Furthermore, E_c was calculated from the experimental $C_{\rm d}$ data by extrapolating to zero thickness for each [OA] (Figure S17, Supporting Information). Plotting E_c versus [OA] revealed a positive linear relationship, meaning that as [OA] increases so does the amount of critical energy required to form a film (E_c) (Figure 5C) making E_c predictable for alternative [OA]'s (Equation 11).

$$E_c = [OA] x + E_c^0 \tag{11}$$

2365709x, 2023, 23, Downloaded from https://onli-

elibrary.wiley.com/doi/10.1002/admt.202300052 by University Of Texas Libraries, Wiley Online Library on [08/05/2024]. See the Terms and Conditions (https://onlinelibrary.wiley.com/

onditions) on Wiley Online Library for rules of use; OA articles are governed by the applicable Creative Commons

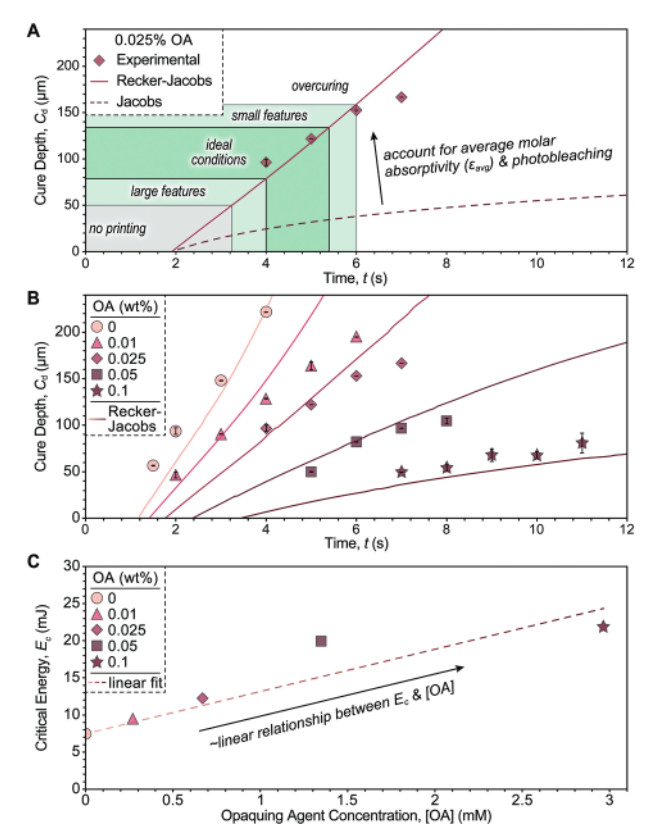


Figure 5. Rheological studies and model fits showing relationships between curing and [OA]. A) Comparing experiment to theory with $C_{\rm d}$ versus. time using 0.025 wt.% OA at an LED intensity of 6.3 mW cm $^{-2}$, showing an improved fit for the Recker–Jacob's equation relative to the original Jacob's equation. Shaded regions represent 3D printing conditions, where shorter and longer exposure times per layer are required to print large and small features, respectively. B) Effect of [OA] on $C_{\rm d}$ with Recker-Jacob's fits. C) Plot of $E_{\rm c}$ versus [OA] showing a positive linear relationship.

where E_c^0 represents E_c for the resin without OA. This finding is in-line with the observation made during prior printing optimization that increasing [OA] necessitated longer exposure times per layer. Based on these results, it was hypothesized that the positive linear relationship between E_c and [OA] within printing relevant concentrations is general for Type II resins, and thus can minimize the number of required rheological measurements to predict optimal printing conditions.

Utility of the Recker-Jacob's equation for optimizing resin formulations and/or 3D printing conditions (e.g., exposure time per layer) requires only a few steps, as outlined in **Figure 6**. Step 1: select the desired light source (wavelength), intensity (*I*), and layer thickness (*I*) for 3D printing. For many commercial light-based 3D printers these parameters are set by the manufacturer or restricted to a specific range. Step 2: measure printer emission profile, unless provided by the manufacturer, and PRC and OA UV-vis absorption profiles. Ideally, absorption should be measured under printing conditions, however dilute solution data will in many cases provide a reasonable estimate and may already be available online for commercial dyes useful as PRCs and OAs (e.g., azo-compounds). At this stage, two resin samples can be prepared, one with no OA, and the other with a user-selected

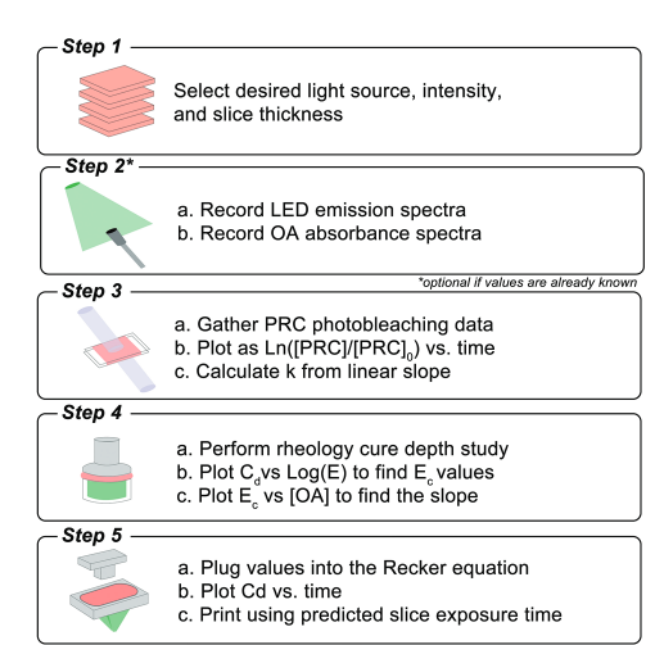


Figure 6. Recommended steps to follow for formulation and printing optimization with a new Type II photocurable resin.

[OA]. A recommended [OA] range is $\approx 0.2\text{-}0.5\times$ [PRC] if avg's of both are within ≈ 1 order of magnitude. Step 3: Collect photobleaching data with a spectrophotometer for the resin without OA and calculate k from the slope of the plot of $\ln(\text{[PRC]/[PRC]_0})$ vs. time. Step 4: Perform photorheology with the two resins (no OA and selected [OA]) under printing conditions to determine relevant C_d values (<500 μ m) for different exposure times (<60 s). Plotting C_d versus E and extrapolating to zero C_d provides E_c values for the two resins, which can be used to determine E_c values for alternative [OA]'s if different exposure times per layer are desired. Step 5: Fill in values for the Recker-Jacob's equation to predict C_d versus time for a given resin composition, which provides an estimate for the ideal exposure time per layer at a given layer thickness.

The Recker-Jacob's equation was tested as a reliable tool for efficiently determining optimal printing parameters by examining an alternative Type II photocurable resin following the steps in Figure 6. Specifically, Rose Bengal was used as the photoredox catalyst in place of EY, and poly(ethylene glycol) diacrylate (PEGDA, $M_n = 700 \text{ g mol}^{-1}$) was used in place of TEGDA as the main resin constituent (crosslinker) (Figure 7A). Although similar in composition, Rose Bengal has a $\lambda_{\rm max}$ that is \approx 40 nm redshifted relative to EY, and PEGDA is considerably more viscous and polar than TEGDA, making this a distinct resin. The other components in the resin were used in the same percentages as discussed previously. For this experiment, the maximum printer light intensity (6.4 mW cm²) was selected, along with a layer thickness of 50 µm (step 1). Next, UV-vis absorption spectroscopy for Rose Bengal in PEGDA:PETMP (99:1) was measured as a thin film between glass slides (step 2), which was used to calculate an $_{avg}$ of \approx 27 000 M 1 cm 1 via Equation 2 for the green LED at 6.4 mW cm² (Figure 7A). Following this, a vial test revealed photopolymerization was both rapid and led to notable bleaching, similar to EY (Figure 7B, inset). Photobleaching was then

2365709x, 2023, 23, Downloaded from https://onlinelibary.wiley.com/doi/10.1002/admt.2023.00052 by University Of Texas Libraries, Wiley Online Library or no [08/05/2024]. See the Terms and Conditions (thtps://onlinelibarry.wiley.com/terms-and-conditions) on Wiley Online Library for rules of use; OA articles are governed by the applicable Creative Commons.

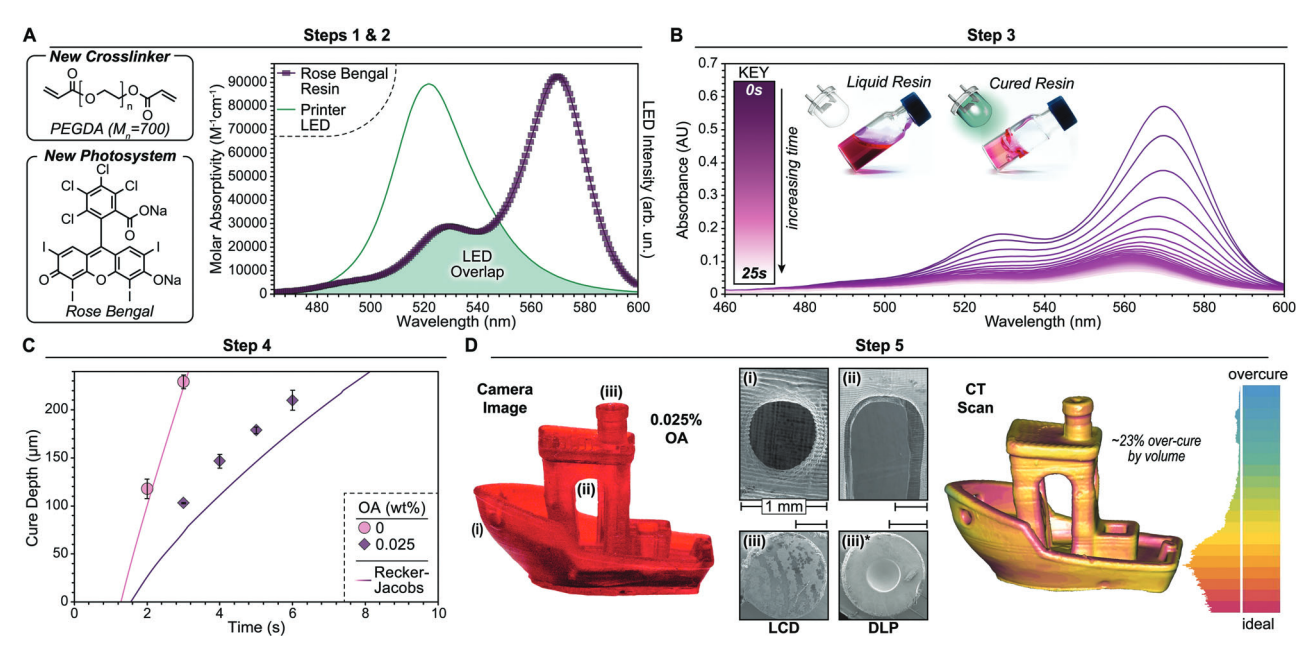


Figure 7. 3D printing optimization using the Recker-Jacob's equation with a distinct resin. A) Chemical structures of crosslinker and photoredox catalyst (Rose Bengal = 0.1 wt.%). Overlay of Rose Bengal absorbance profile, obtained in PEGDA:PETMP (99:1) resin, with printer green LED profile; overlapping area shaded in green. B) UV-vis absorbance plot of a resin containing Rose Bengal and Oil Red O (0.025 wt.%) upon exposure to a green LED at 6.3 mW cm². Inset vials showing pre- (top) and post- (bottom) green LED exposure. C) Photorheological cure depth study and the Recker-Jacob's working curve. D) Calibration test print of "3DBenchy" produced using 0.025 wt.% OA resin at an intensity of 6.3 mW cm², showing camera image (left), corresponding SEM images (center), and reconstructed 3D image from CT scans (right). The colored bar represents over-cure generated by overlaying the CT scan and digital print file, with the histogram showing normalized distances of printed voxels from their digital position. SEM images (iii) and (iii)* represent the "smokestack" on 3DBenchy's printed using LCD and DLP, respectively.

quantified for the new resin containing no OA and 0.025 wt.% OA (step 3). Plotting the [Rose Bengal] versus t and following Equation 5 provided the photobleaching rate constant, k, along with a relationship to intensity of 0.028I, under the assumptions made for Equation 9 (Figure 7B and Figure S85, Supporting Information). For the same [OA]'s, rheology was used to determine C_d at a few different exposure times per layer (step 4), which provided E_c using Equation 11 (Figure S86, Supporting Information), and showed good agreement with the theoretical Recker-Jacob's working curve (Figure 7C). Based upon this data and a theoretical C_d of $\approx 100 \mu m$, the optimal exposure time was determined to be 3.5 s per layer, which was used to print 3DBenchy (step 5) (Figure 7D). Both SEM images and volume analysis from CT confirmed good print fidelity (high resolution), with an overcure of ≈23% by volume (Figure 7D), similar to the "3Dbenchy" produced using empirically optimized conditions (Figure 3D). Furthermore, it was demonstrated that the optimal parameters for green light LCD 3D printing translated effectively to green light DLP 3D printing, with only ≈15% over-cure by volume (Figure 7D and Figures S91-S95, Supporting Information). This decrease in over-cure for DLP relative to LCD 3D printing was attributed to the inherently higher resolution of the DLP system (1 pixel = $21 \mu m$).

3. Concluding Remarks

In this study, green light ($\lambda_{\rm max} \approx 525$ nm) LCD 3D printing was accomplished for the first time, and a streamlined process for optimizing visible light projection-based 3D printing was development.

oped. The optimization method arose from a systematic examination of factors that influence both speed and resolution of 3D printing, namely light intensity, photosystem absorbance, and photo-polymerization and -bleaching kinetics. This culminated in a modified cure depth (C_d) model termed the "Recker–Jacob's equation", which correlates resin composition to optimal printing conditions (e.g., exposure time per layer). The model was incorporated into a five-step 3D printing optimization protocol that only requires basic optical measurements of light source emission and resin absorption profiles, together with minimal measurements of C_d using a rheometer. This protocol was verified using a distinct green-light activated resin, which quickly provided the optimal exposure time per layer for LCD 3D printing. High fidelity printing was accomplished for a resolution calibration file, 3DBenchy, using the optimized conditions, as confirmed by both SEM and CT scanning. Future modifications to consider for further improving the accuracy of the model include quantification of secondary effects, such as heat from polymerization and/or the LEDs. The insights into visible light photocuring processes presented herein, along with the associated 3D printing optimization protocol, are anticipated to accelerate the discovery and implementation of next generation visible light activated photosystems for advanced manufacturing of functional plastics.

Supporting Information

Supporting Information is available from the Wiley Online Library or from the author.